

Catalytic activity of gold-perovskite catalysts in the oxidation of carbon monoxide

Leboheng Mokoena¹ · Gary Pattrick² · Mike S Scurrell³

Received: 5 January 2016 / Accepted: 5 June 2016
© Springer International Publishing Switzerland 2016

Abstract Perovskites (ABO_3 structures), which can be manipulated by partial substitution, are reported to be active supports for CO oxidation, but only at high temperatures, with no activity being shown for temperatures below 200 °C. In this study, these perovskites were investigated at low temperatures (below 100 °C) with improved activity found upon gold deposition. The presence of gold nanoparticles therefore significantly enhanced the catalytic activity, while the support itself was suspected to be involved in the reaction mechanism. A series of perovskites of the type ABO_3 ($LaMnO_3$, $LaFeO_3$, $LaCoO_3$, and $LaCuO_3$) were prepared using the citrate method, while the gold was deposited on them using the deposition-precipitation method. The supports were calcined at different temperatures for optimization. With the support calcined at 800 °C, the best catalyst was 1 wt% Au supported on $LaFeO_3$. Calcium-doping of this system showed decreased surface area, poorer crystallinity, and a drop in catalytic activity relative to the Au- $LaFeO_3$. In addition, Au- $LaFeO_3$ showed online stability over 21 h. Calcining the support improved the incorporation of gold nanoparticles into the perovskite lattice, resulting in superior catalytic activity. Nevertheless, at higher calcination temperatures, the catalytic activity of Au- $CaTiO_3$ was depressed while that of Au- $LaFeO_3$ was enhanced. XPS revealed that in the active catalysts, both cationic and metallic gold coexisted, while in the

inactive catalysts, the gold existed predominantly either as cationic or metallic gold.

Keywords Gold · Perovskites · CO · Oxidation · Lanthanum · Iron · SIMS · XPS

Introduction

Perovskites, ABO_3 represent an interesting type of solid known for their catalytic action, photovoltaic applications and for their catalytic role in providing supports for metals [1, 2]. They have been fairly well studied for oxidation reactions. The $La_{1-x}Sr_xO_3$ system has been reported to rival commercial platinum catalysts for NO oxidation in simulated diesel exhaust [3]. A very recent and detailed appraisal of the potential of perovskites as substitute catalysts for noble metals has been given [4]. The overall conclusion is that despite intense efforts to improve the catalytic activity of perovskites, they are more likely in the short term to be useful as supports for noble metals as a means of enabling the use of lower precious metal loadings and extending catalyst life. Gold has been much studied for a variety of catalytic reactions, most notably for the low temperature oxidation of carbon monoxide, following the pioneering work carried out by Huratu and his group [5–13]. Supports are normally metal oxides, such as alumina or reducible oxides such as titania, iron oxide, and cobalt oxide. Palladium-perovskites have been the subject of studies for potential use in automotive exhaust systems and appear to offer the property of self-regeneration, associated with palladium's ability to move in or out of the perovskite structure depending on the oxidizing/reducing characteristics of the atmosphere [11, 12]. Systems studied include $LaFe_{0.57}Co_{0.38}Pd_{0.05}O_3$ [11] or the simpler composition $LaFe_{0.95}Pd_{0.05}O_3$ [12]. Another interesting system,

✉ Mike S Scurrell
scurrms@unisa.ac.za

¹ Molecular Sciences Institute, School of Chemistry, University of the Witwatersrand, Johannesburg 2050, South Africa

² MINTEK, Johannesburg, Randburg 2125, South Africa

³ Department of Civil and Chemical Engineering, University of South Africa, Johannesburg, FL 1710, South Africa

$\text{La}_{0.8}\text{Sr}_{0.2}\text{MnO}_3$ was shown to exhibit higher stability and activity for the total combustion of toluene if gold were added [14], related to an increased surface oxygen mobility and the resulting solids were of comparable activity to that of palladium/alumina. One other study of a gold-perovskite system has been published [15] and reports that the specific catalytic activity for CO oxidation is about two orders of magnitude lower than found with the more extensively studied gold-titania catalysts [5–13]. Other papers have examined gold-perovskites and reported the essential catalytic data for CO oxidation [16]. A combinatorial study mentioned gold among several noble metals and perovskites [17] but the most active catalysts found for CO oxidation contained neither. Our state of knowledge about gold-perovskites is therefore extremely limited. In particular, almost no characterization work has been carried out beyond XRD, textural studies and some XPS work which suggest that metallic gold coexists with ionic gold species, with the latter apparently aiding catalytic activity [16]. More detailed characterization work is unavailable as is the exploration of the powerful ability of perovskites to be modified by substituting other cations in gold systems for CO oxidation. In this paper, we have addressed these issues. Two perovskite systems, CaTiO_3 and $\text{LaCa}_x\text{FeO}_3$ (short for $\text{LaCa}_x\text{Fe}_{1-x}\text{O}_{3-0.5x}$), were selected in order to check if any major differences are displayed for different perovskites when used as a support for gold in catalysis. We have employed a citrate-based method for the synthesis of some of these solids. The citrate-based complexing process, a modified Pechini-type reaction, is a polymerized complex method to synthesize a wide variety of oxide materials [18]. Various metal ions in a solution are chelated to form metal complexes and then these chelates undergo polyesterification reactions when heated to form a glass which has metal ions uniformly distributed throughout [19, 20]. Thereby, the resultant powders have a nanoscale particle size and high compositional homogeneity at the molecular level.

Experimental

HAuCl_3 (Sigma-Aldrich, 99.99 %) was used as the precursor for the Au nanoparticles. Sodium borohydride [NaBH_4] (Fluka Chemie) was used to reduce Au^{3+} and ammonium hydroxide [NH_4OH] (SAARCHEM), diluted to 12.5 % using distilled water was used to maintain the pH at around 8–8.5 during the preparation of the Au catalyst. (Although some have cautioned against the use of ammonium hydroxide in this way because of the potential for the formation of explosive gold fulminate, we have never experienced any problems when working carefully with this reagent and this method does avoid the use of alkali metals which can influence activity [11].) The intended gold loading was 1.0 wt% with respect to the support. TiO_2 (P25, Degussa) containing 80 % of anatase and 20 % of rutile phases and calcium nitrate [Ca

$(\text{NO}_3)_2 \cdot 3\text{H}_2\text{O}$] (SAARCHEM, 99 %) were used for the preparation of CaTiO_3 . Lanthanum nitrate [$\text{La}(\text{NO}_3)_3 \cdot 6\text{H}_2\text{O}$] (Merck, 99 %), iron nitrate [$\text{Fe}(\text{NO}_3)_3 \cdot 3\text{H}_2\text{O}$] (SAARCHEM, 99 %), citric acid (Sigma-Aldrich, 99 %), and $\text{Ca}(\text{NO}_3)_2 \cdot 3\text{H}_2\text{O}$ (SAARCHEM, 99 %) were used for the preparation of $\text{LaCa}_x\text{FeO}_3$. All the chemicals were used as received without any further analysis or purification. The following gas mixtures obtained from AFROX were used for the CO oxidation, He, 99.999 %, 10 % O_2 and 5 % CO.

CaTiO_3 was prepared by a method of hydrothermal synthesis. $\text{TiO}_2 \cdot x\text{H}_2\text{O}$ was used as a source of Ti and commercial $\text{Ca}(\text{NO}_3)_2 \cdot 4\text{H}_2\text{O}$ used as a source of Ca. 30 g of TiO_2 and 89 g $\text{Ca}(\text{NO}_3)_2 \cdot 4\text{H}_2\text{O}$ were charged into the stainless steel Teflon-lined autoclave along with 200 ml of deionized water. The pH was adjusted to 13 using KOH. The reaction time was 12 h at the stirring rate of 2 and heated at 160 °C. The stirring was stopped after 12 h and the solution was allowed to age for 48 h. The solution was washed for approximately 1 week until the conductivity was $4.3 \times 10 \mu\text{S}$. The product was dried at 110 °C for 4 h. It was then calcined at 400, 600, or 800 °C overnight.

$\text{LaCa}_x\text{FeO}_3$ (where x corresponds to 0, 4, 10, 16, or 20 wt%) was prepared by the citrate method [21]. Iron nitrate, lanthanum nitrate, citric acid and/or calcium nitrate were dissolved in deionized water and heated at 100 °C overnight in an oil bath then calcined at different temperatures (400, 600, or 800 °C for $x = 0$ samples and 800 °C for $x = 4, 10, 16,$ or 20 % samples) for 1 h.

Au-CaTiO_3 was prepared by the single step borohydride method. The support was suspended in distilled water (200 ml) and stirred vigorously. A required amount of diluted HAuCl_4 solution ($10^{-2} \text{ moldm}^{-3}$) was slowly added with continuous stirring. The pH of the solution was maintained at 8.5 by adding 15 % NH_4OH dropwise under the same conditions. The precipitated solution was aged for 2 h. A solution of NaBH_4 prepared in ice water was added in the required amount rapidly to ensure the complete reduction of Au(III) to Au(0). The suspended solution was then aged for a further 2 h, filtered and dried at 120 °C for 4 h. Samples were calcined at 300 °C for 4 h and then stored.

The Au- $\text{LaCa}_x\text{FeO}_3$ catalysts were prepared by the deposition-precipitation method. The support was suspended in deionized water (200 ml) and the required amount of HAuCl_4 added dropwise then stirred for 2 h. 15 % NH_4OH was then added to adjust the pH to 8.5 then stirred for a further 2 h. The catalyst was then filtered and washed with hot water then dried in the dark overnight. Samples were calcined at 300 °C for 4 h and then stored.

Catalytic activity was measured using a fixed bed flow reactor. Catalyst (undiluted) (100 mg) was placed in a Pyrex glass reactor, heated to 300 °C for 2 h in a stream of oxygen (10 % oxygen, balance He) at a flow rate of $40 \text{ cm}^3 \text{ min}^{-1}$. A mixture of oxygen and carbon monoxide

(5 % CO, 10 % O₂, balance He) was admitted at a flow rate of 40 cm³ min⁻¹ through the reactor after it had been cooled to room temperature, 20 °C. The exit stream was analyzed by two columns using gas chromatography (5710A GC, Hewlett Packard). Conversion was assessed usually in terms of CO loss, but confirmed sometimes by the determination of CO₂ produced.

The surface area of the catalysts was determined using a Micromeritics ASAP 2010 porosimeter.

Powder X-ray diffraction data were collected via a Bruker AXS D8 diffractometer using Cu-K α radiation (40 kV, 40 mA) equipped with a primary beam Gobel mirror, a radial Soller slit, and a Vantec-1 detector. Data were collected in the 2 θ range of 5 to 90° in 0.021° steps, using a scan speed resulting in an equivalent counting time of 14.7 s per step.

Raman spectra were acquired with a Jobin-Yvon T64000 Raman spectrometer operated in single spectrograph mode. Excitation was by means of the 514.5 nm line of an argon ion laser. It was focused onto the sample via an Olympus microscope attachment and the collected light was dispersed onto a liquid nitrogen-cooled CCD with an 1800 line/mm grating. For the AuCaTiO₃ samples, a 20 \times objective was used and for the LaFeO₃ samples a 50 \times objective was used. Laser power at the sample was kept to ~1.2 mW to prevent localized heating. Data was collected with Lab Spec 4.18 software and acquisition times varied from 120 to 180 s.

Powdered samples were suspended in ethanol with sonication treatment for a few minutes to allow for the evaporation of ethanol before the grid was inserted into the instrument.

X-ray photoelectron spectra were measured on a Kratos Axis Ultra DLD spectrometer using a monochromatic AlK α X-ray source (75 W) and an analyzer pass energy of 160 eV for survey spectra and 40 eV for detailed scans. Samples were mounted using double-sided adhesive tape, and binding energies are referenced to the C(1s) binding energy of adventitious carbon contamination taken to be 284.7 eV. Data were analyzed using commercial software (CasaXPS; Neil Fairley) and software developed in-house at Cardiff University.

A time of flight Secondary Ion Mass Spectrometer (ION TOF), housed at the National Metrology Institute of South Africa (NMISA) in Pretoria, was used for data collection. The sample powders were pressed onto indium foil and analyzed as is. A 25 kV Bi⁺ ion beam with a pulsed current of 1 pA and a rate of 10 kHz was used. The extractor was operated at 2 kV and charge neutralization was applied. The beam diameter was 1 μ m and the analysis area was 100 \times 100 μ m (128 \times 128 pixels).

The actual gold content of the catalysts were measured using fire assay for total gold followed by gravimetric finish by Performance Laboratories in Randfontein, and were close to the target value of 1 wt%.

Results and discussion

Catalytic measurements

Systems that were investigated included gold supported on LaFeO₃, LaMnO₃, LaCoO₃ and LaCuO₃ perovskites. Only catalysts supported on CaTiO₃ and LaFeO₃ showed activity for reaction temperatures below 100 °C for which reason the other perovskites (i.e., LaMnO₃, LaCoO₃, and LaCuO₃) were eliminated from the study.

Figure 1 shows the activity measurements for Au-CaTiO₃ towards CO oxidation.

Figure 2 shows the stability measurements for Au-CaTiO₃ towards CO oxidation.

There is an increase in conversion as the calcination and reaction temperature is increased, but there was no activity for samples calcined at 800 °C under the investigating conditions. There was an initial high activity for all catalysts but deactivated gradually over time.

Figure 3 shows the activity measurements for Au-LaFeO₃.

The stability of this system is depicted in Fig. 4.

There is an increase in activity as the reaction temperature increases also as the calcination temperature increased but a decrease with the sample calcined at 800 °C. As the time on stream is increased, there is an initial increase in activity for the samples calcined at 400 and 600 °C but the sample at 800 °C remains stable throughout.

The activity measurements for LaCa_{*x*}FeO₃ (where *x* corresponds to 0, 4, 10, 16, or 20 w% Ca) towards CO oxidation at atmospheric pressure as a function of temperature is shown in Fig. 5.

The TOF values at 30 °C for the Au-LaFeO₃ and Au-CaTiO₃ are 0.09 and 0.04 s⁻¹, respectively, based on total contained gold, some 30 or 13 times higher than the values reported for Au-LaSrMnO₃ [15]. Changes in increasing activity seen with the lower calcium content samples (Fig. 6) may therefore be indicative of changes occurring in the surface distribution or form of calcium during the early stages of the oxidation reaction. There may be an additional role for calcium in helping to capture carbon dioxide during the oxidation reaction though this specific aspect cannot be discerned from the data alone. Further, more detailed studies of the surface chemistry of the catalysts as a function of time on stream are planned and could help in furthering our understanding of the situation. There is a tendency for activity to increase as the time on stream increased. The catalysts with 4 and 10 % calcium loading had an initial increase in activity (Fig. 7), suggesting that some sort of activation process was taking place then stabilized while the 16 and 20 % samples showed an increase followed by a stabilization. The calcium-free sample showed stable behavior throughout the period of time investigated. In general, even in the absence of additional calcium, the AuFeTiO₃ is noticeably more stable than the Au-CaTiO₃

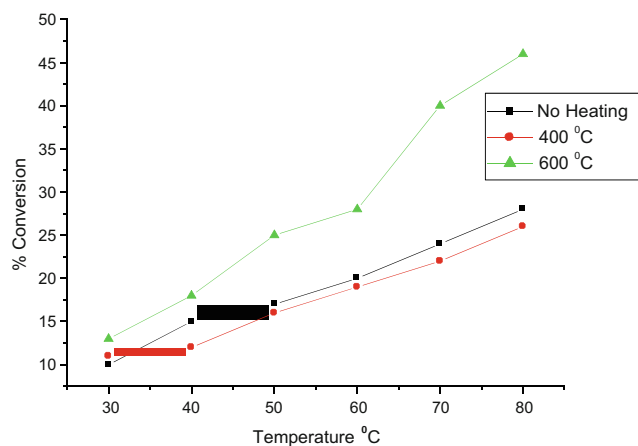


Fig. 1 CO conversion over Au-CaTiO₃ at different temperatures

catalyst, another feature that is worth examining more closely. The former catalysts show hardly any deactivation over a 24-h period on stream.

Increasing temperature of calcination and increasing gold loading reduced the specific surface area (Table 1). For LaFeO₃, the calcination increases the surface area and gold loading decreases the area except for the 400 °C sample when gold loading increased the surface area. The reason for this behavior is unclear. When LaFeO₃ is doped with Ca, the surface area decreases (from 25.4 to 17.5 m²/g). The specific surface area again increases upon incorporation with gold, particularly for the higher Ca content samples. These increases in surface area may be the result of some etching of the perovskites. Hydrothermal treatment with water alone has been shown to result in increased specific surface area of perovskite samples [22]. Perovskites of the type LaBO₃ (B = Co, Ni, Mn) have been reported as having specific surface areas in the range 33–44 m²/g [23]. All our perovskites prepared had low to medium specific surface areas. The calcium amount detected is in agreement with the theoretical value except for

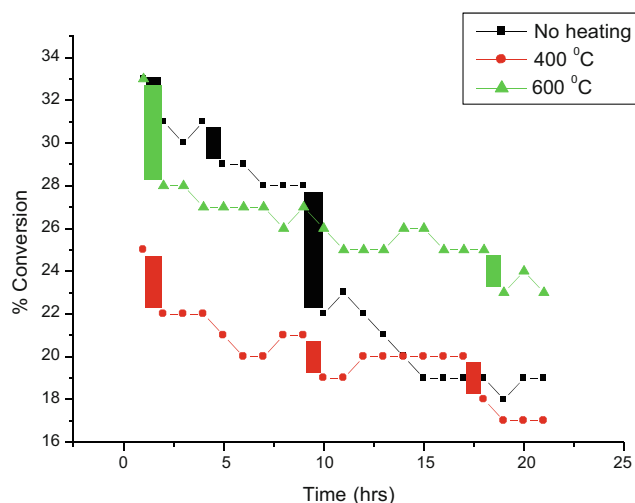


Fig. 2 CO conversion over time at a reaction temperature of 20 °C over the Au-CaTiO₃

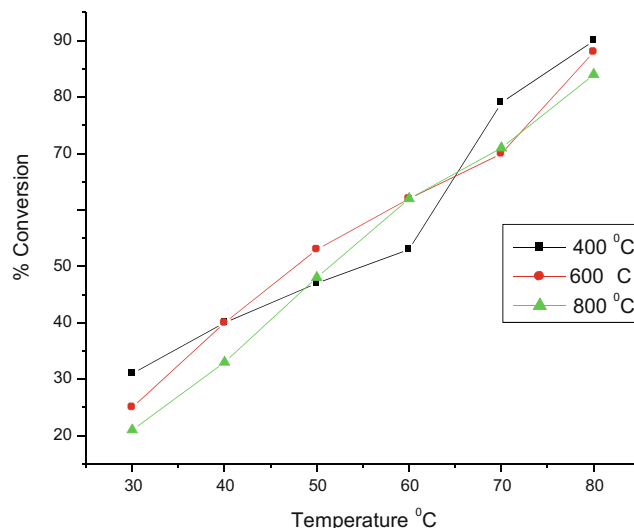


Fig. 3 CO conversion over Au-LaFeO₃ at different temperatures

the expected 20 % loading which is much lower. The reason for this is unlikely to be that the calcium level is approaching the maximum value of 28 % for a zero-lanthanum content perovskite, with 20 % Ca corresponding to a composition of La_{0.17}Ca_{0.83}FeO₃. No phase changes for the perovskites are expected for the temperature range investigated. It is likely that phase transitions would occur only at significantly higher temperatures [24], though there might be some oxygen loss from the lattice at higher calcination temperatures [25].

XRD, XPS, and Raman characterization

All the perovskites formed were pure phase and calcination did not normally change the structure of the different perovskites (Figs 8, 9, and 10). The exception is with the calcium loaded samples, where there is a decrease in peak intensity as

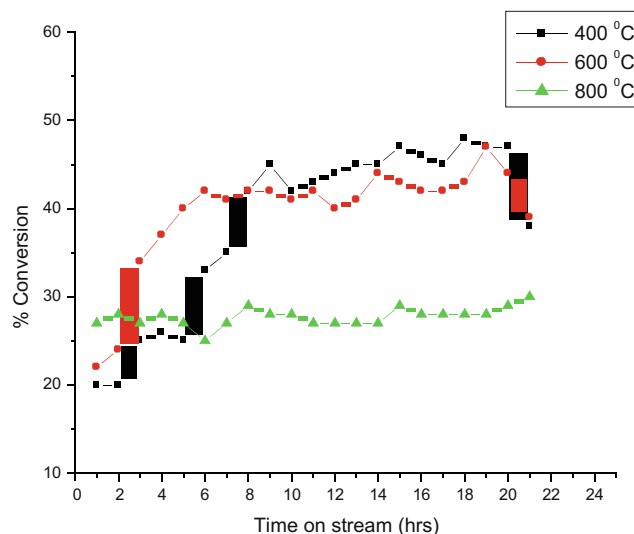


Fig. 4 CO conversion over time at a reaction temperature of 20 °C for Au-LaFeO₃

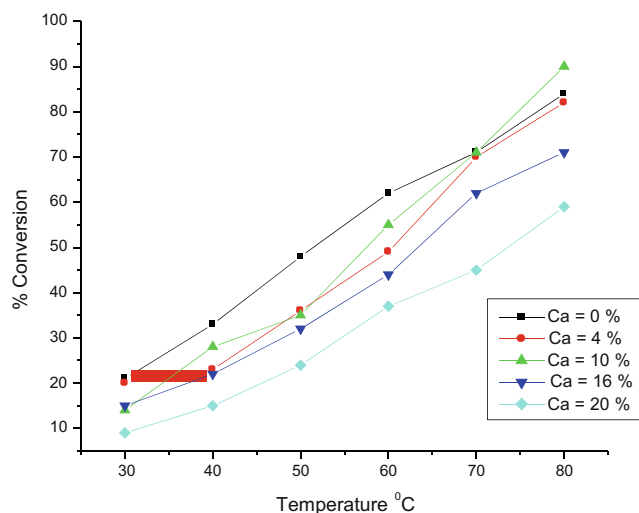


Fig. 5 CO conversion over $\text{LaCa}_x\text{FeO}_3$ at different temperatures

the calcium loading is increased and some shift to higher 2θ values as the Ca content is increased. In addition, some peaks disappear at high calcium loadings. Gold could not be detected as the gold peaks overlapped with the support peaks and the loading was too low. The expected peak near $2\theta = 63^\circ$ was not visible and this alone suggests that the gold was very highly dispersed in the samples.

From XRD and Raman spectroscopy (Fig. 11), it is evident that the support was formed at the different calcination temperatures with an increase in crystallinity as the calcination temperature is increased. The activity increased with both reaction and calcination temperature up to 600°C , the support calcined at 800°C showed no activity under the investigating conditions. It is reported in literature that the higher the surface area the more active the catalyst, also Ti ions have been shown to be the active sites for Ti-based catalysts. The support calcined at 800°C had the lowest surface area and the interaction

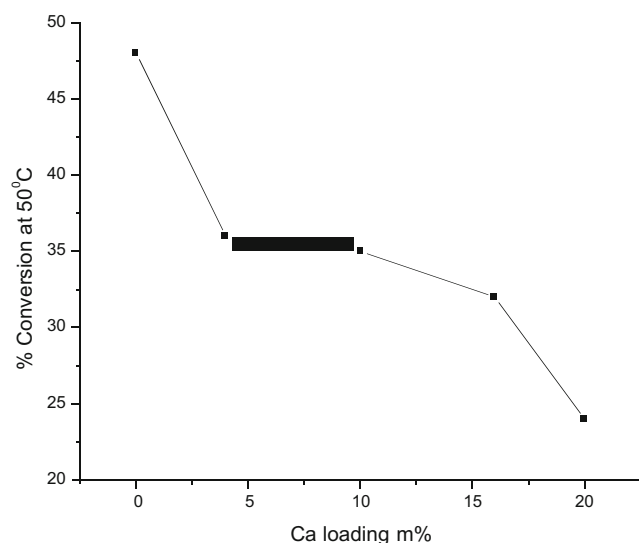


Fig. 6 Graph showing effect of calcium loading on CO conversion measured at 50°C

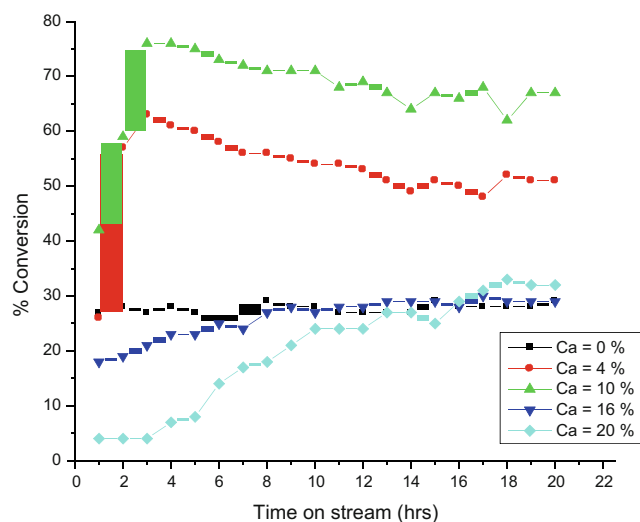


Fig. 7 CO conversion at 40°C over time for $\text{LaCa}_x\text{FeO}_3$

between Ti and Au was the lowest for this sample, therefore the resulting loss in activity. These % conversion results correlate with the XPS analysis (Fig. 12), the intensity of the Au(4f) peak decreases as calcination temperature is increased as shown in Table 2. This can be due to the incorporation of the Au into the perovskite lattice calcined at higher temperatures which results in better interaction of the gold and the support (shown by the shift in binding energy) therefore improved activity. The Ca(2p) peaks did not shift in binding energy or intensity, only the O(1s) had subtle changes which could reflect different coverage of hydroxyl or carbonate species.

The surface area decreased as the calcination temperature increased which is expected, and it also decreased upon gold loading. These catalysts were found to gradually deactivate over the period of time investigated, i.e., in 5 h there was ± 8 percentage units decrease in conversion.

Table 1 Specific surface areas for the various catalysts calcined at 300°C

Support	Temperature or loading	Without Au (m^2/g)	With Au (m^2/g)
CaTiO ₃	No heating	45.1	13.3
	400 °C	41.7	12.8
	600 °C	34.4	12.7
	800 °C	10.1	10.3
LaFeO ₃	400 °C	14.2	39.1
	600 °C	19.3	15.0
	800 °C	25.4	9.1
LaCaFeO ₃	Ca = 4 % (3.5) ^a	17.5	17.7
	10 % (10.1)	14.9	17.0
	16 % (16.8)	14.3	24.4
	20 % (16.7)	17.5	53.3

^a Values in brackets are the calcium composition from XRF

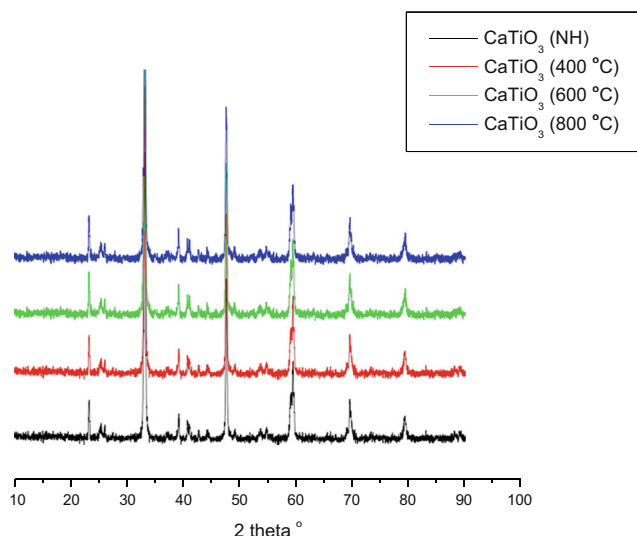


Fig. 8 Diffractograms for CaTiO_3 calcined at different temperatures

The XPS analysis for LaFeO_3 was complex, with two doublets corresponding to Au^0 and Au^{3+} species for the Au(4f) region. As the calcination temperature was increased, it led to more cationic species being formed with their intensity decreasing as the temperature was increased.

The reduction in intensity corresponds with the increase in activity as the calcination temperature was increased. This means that as the calcination temperature is increased, there is more extensive incorporation of the gold into the support. In palladium-perovskites, there is clear evidence that palladium can occupy the B sites (6-fold coordination) the ionic radii of gold (Au^{3+}) and palladium (Pd^{2+}) are very close at 82 and 78 pm, respectively, and so it is tempting to speculate that gold may behave similarly. (It is noted that no XRD peaks due to palladium metal were seen in the Pd-perovskites for a

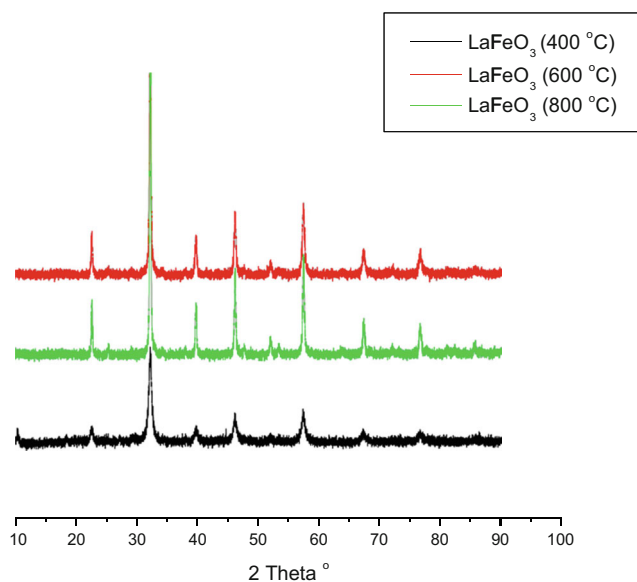


Fig. 9 Diffractograms for LaFeO_3 at different calcination temperatures

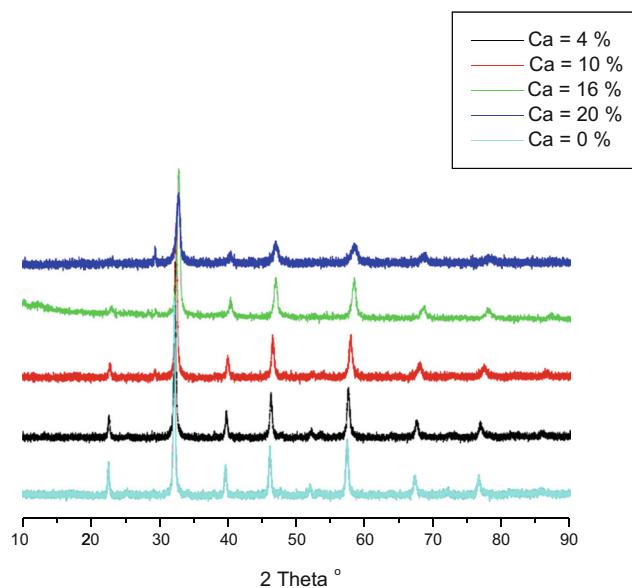


Fig. 10 Diffractograms showing effect of calcium loading on LaFeO_3 for samples calcined at 300 °C

Pd content of 5 atom% [26]. For $\text{LaCa}_x\text{FeO}_3$, the cationic gold species was transformed into the metallic gold as the Ca loading was increased. The intensity of these samples decreased with the 16 and 20 % Ca loading. The Ca(2p) spectra show dramatic differences as a function of Ca loading (Fig. 16). In contrast to the Au- CaTiO_3 samples (Fig. 14), the Ca(2p) spectra exhibit two components, the higher binding energy component increasing in relative intensity as the Ca loading increases. The total Ca(2p) intensity increased with Ca loading up to 16 %; the intensities for the 16 and 20 % samples are very similar. Presumably, this represents Ca species in two

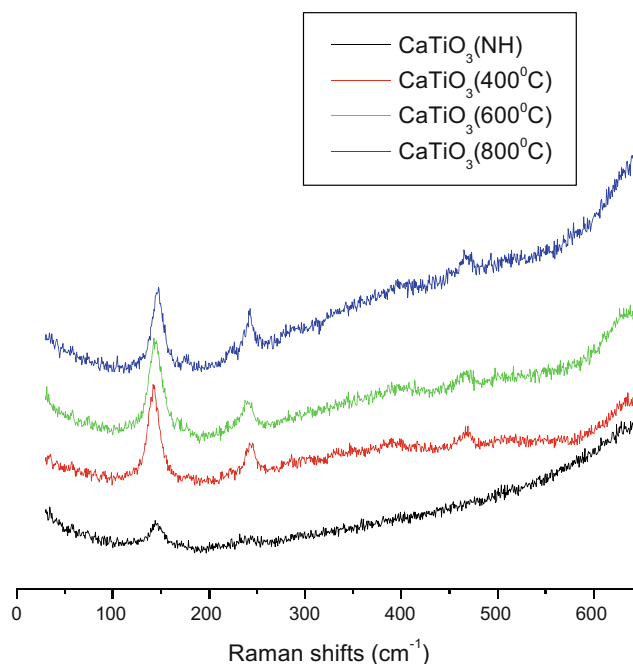


Fig. 11 Raman spectra for CaTiO_3 calcined at different temperatures

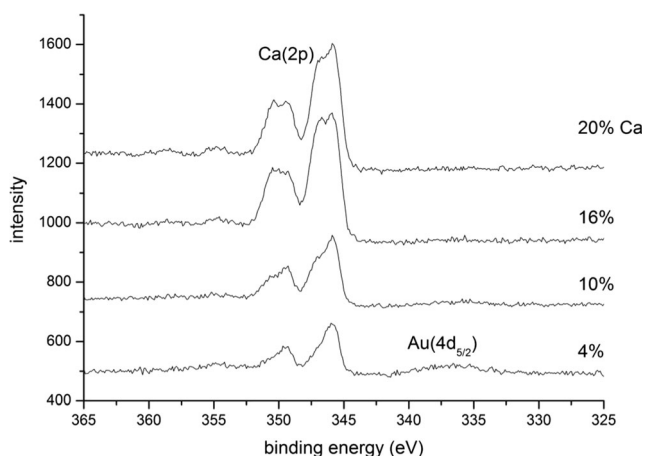


Fig. 12 Spectra showing Ca(2p) binding energies for Ca doped-LaFeO₃

different environments or lattice positions, a conclusion supported by the La(3d) spectra (Fig. 10), where the spectra corresponding to 16 and 20 % Ca loadings show evidence for two La states in the broadening of the signals, reflecting different interactions between the La and Ca atoms. The fact that gold is present in two oxidation states may also be relevant here. For the 16 and 20 % Ca samples, there is a large increase in the high binding energy component of the O(1s) peaks compared with the samples with lower Ca loadings, possibly reflecting the contribution from “CaO” species to the O(1s) envelope, although the relative intensity of this high binding energy feature appears to be too high. However, it is clearly correlated with the observations made in the Ca(2p) and La(3d) signals concerning different Ca species or Ca entities present in different environments.

XRD investigations revealed the presence of pure and crystalline phases for all the prepared perovskites. No secondary phases could be detected by this method at least within the precision limits of this technique. Substitution of Ca for La resulted in the XRD diffraction lines being broadened, shifted slightly to higher 2θ values and their intensities decreasing as the Ca amount was increased. This is due to the Ca inducing changes in the crystalline structure modifying the orthorhombic structure to a nearly cubic structure. This was also supported by the analysis from Raman spectroscopy which revealed bands for the unsubstituted LaFeO₃ but with no bands

being observed for the substituted perovskite, in line with the absence of Raman bands for cubic symmetry [27].

It has been reported that substitution of La by Ca causes a decrease in the cell volume which can be seen from the shift in XRD diffraction lines. Calcium has a lower oxidation state than lanthanum and therefore to maintain the structure electroneutrality, an increase takes place in the iron oxidation state from Fe³⁺ to Fe⁴⁺. Since the latter has a smaller ionic radius, the cell volume is decreased. In the Fe based perovskite, Fe⁴⁺ ions have been reported [28, 29] to be the active sites for oxidation reactions.

From SIMS measurements, there is evidence that substitution of Ca for La results in less direct contact between Au and Fe entities. The direct interaction between Au centers and the active Fe ions is not seen as Ca is loaded (certain Fe probable species present in the samples without Ca are not present in the samples with Ca, i.e., FeAu and Fe₃AuO instead CaAu is present). Also the intensity of FeAuO and LaFeO₂ species decrease as Ca loading is increased. Yakovleva and her colleagues [30] showed based on their SIMS data for LaCa_xMnO₃ that there is surface segregation of Ca and thereby blockage of part of the active sites on the surface. Therefore, we can therefore assume that due to the lack of Au-Fe interaction and increased interaction between Au and Ca, the active sites are blocked, leading to a reduction in activity, as observed, as the calcium loading is increased. The interaction between Au and Ca is also considered to be responsible for the fall in surface abundance of gold as clearly revealed in the XPS spectra of highly Ca-loaded samples.

For all catalysts, there was a decrease in initial activity with time on stream and this is due to a progressive self-poisoning effect, probably due to the strong adsorption of the products (CO₂ and/or carbonates species) at low temperatures. In conclusion, the citrate method was successful in preparing the different perovskites and the deposition-precipitation method in depositing the gold onto the supports. Calcining at different temperatures increased the incorporation of the gold into the support which resulted in higher activity except for the CaTiO₃ where calcination at 800 °C resulted in less interaction between Au centers and the Ti active species. Cationic gold species are found in all the active catalysts while metallic gold was found in the inactive catalysts. These catalysts were reasonably stable but had low % conversions therefore improving the activity would be beneficial since they are promising materials. At low reaction temperatures, all catalysts had an initial increase in activity which decreased as a result of self-poisoning with time on stream. Modification with Ca did not improve the catalytic performance but instead decreased it dramatically as the Ca loading was increased. Doping the support with Ca led to blockage of the active sites which led to reduced catalytic activity. Corresponding perovskites without gold were not active and therefore the presence of gold nanoparticles significantly enhanced the activity but the

Table 2 Surface compositions for Au-CaTiO₃

T(calcined) °C ^a	Composition at%				Elemental ratios	
	O	Ti	Ca	Au	O/(Ti + Ca)	Au/Ti
Uncalcined	60.7	14.9	21.5	2.9	1.67	0.19
400	64.5	17.6	17.3	0.6	1.85	0.03
600	58.7	24.5	16.2	0.6	1.44	0.02
800	65	18.2	16.4	0.5	1.88	0.03

^a Calcination was carried out before the addition of Au

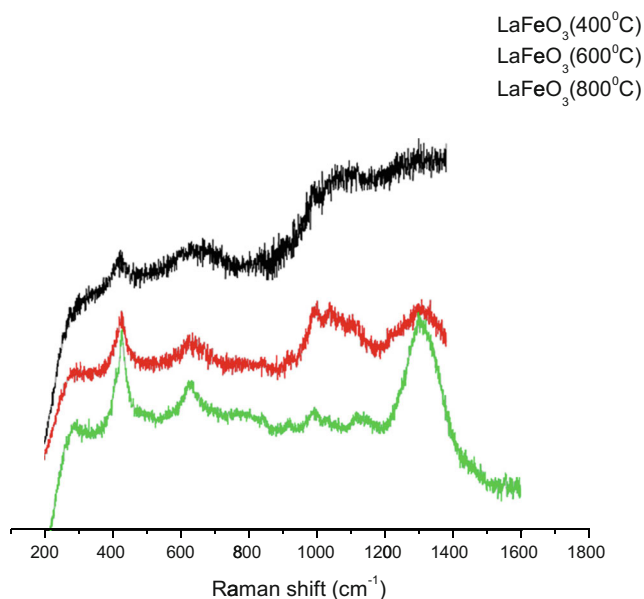


Fig. 13 Raman spectra for LaFeO_3 at different calcination temperatures

support itself plays a key role in the reaction. The absolute rates of CO oxidation are comparable with the acknowledged very active Au-titania systems. At 300K, we find a TOF of close to $0.03 \text{ mol}_{\text{CO}}\text{mol}_{\text{Au}}^{-1}$, based on total Au contained, identical to the value reported by Costello et al. [31, 32] and others [11] for the titania-supported system.

Only very few Raman spectra for LaFeO_3 perovskite have been reported [27], but these are similar to the spectra obtained for our samples. Raman spectroscopy was used to study the crystallinity of the materials by looking at peak height and peak broadening of characteristic absorptions. It is reported in the literature that amorphous materials show broad Raman peaks. Figure 13 shows the observed spectra. The supports calcined at 400 and 600 °C were observed to be more crystalline as their peaks were more pronounced and intense. The 142 cm^{-1} P1 Raman mode is related to the CaTiO_3 lattice

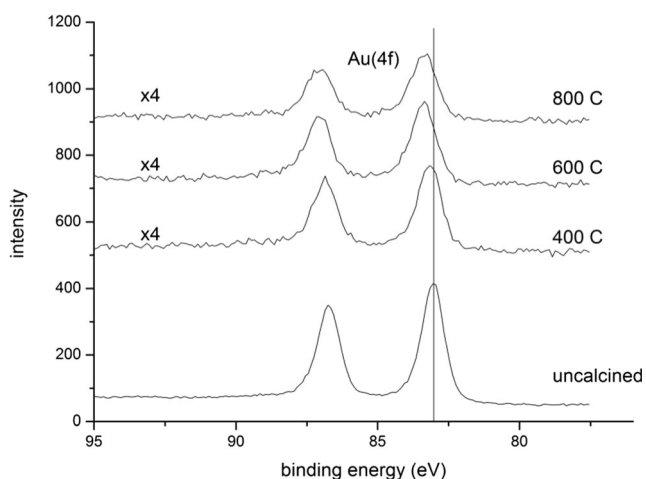


Fig. 14 Spectra showing Au (4f) binding energies for CaTiO_3

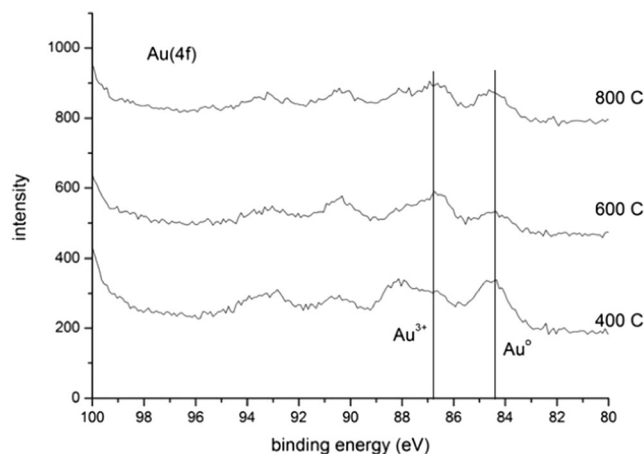


Fig. 15 Spectra showing Au (4f) binding energies for LaFeO_3

mode at 241 cm^{-1} P4 which is the O–Ti–O bending mode. The 467 cm^{-1} peak P7 is ascribed to the torsional mode.

Little work has been done on the calculation and assignments of the Raman modes for LaFeO_3 (see Fig. 13). Moreover, there are some controversial points in the assignments of the modes [28]. For example, the band at $\sim 625 \text{ cm}^{-1}$ was assigned to two phonon scattering mode in ref. [5] and the same band was assigned to impurity related scattering mode elsewhere [6]. In this work, Raman spectroscopy was used to support the XRD data to determine whether crystallinity plays a role in the activity of these materials by considering the peak intensity and peak broadening. The peak intensity increased with an increase in calcination temperature meaning that crystallinity increased when the sample was calcined at higher temperatures. The 431 cm^{-1} peak arises from the B3g mode and that at 628 cm^{-1} from two phonon/impurity scattering. Peaks at 991, 1129, and 1306 cm^{-1} all arise from two phonon scattering processes. There is an increase in crystallinity of the samples as the calcination temperature is increased for both CaTiO_3 and LaFeO_3 perovskites. Modification of LaFeO_3 with Ca decreases the crystallinity drastically so that no peaks were observed for all the Ca doped- supports in the Raman region where presented featureless profiles.

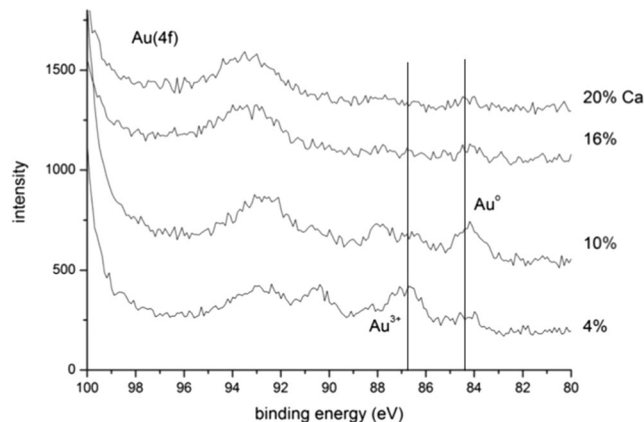


Fig. 16 Spectra showing Au (4f) binding energies for Ca doped LaFeO_3

Table 3 Data from SIMS analysis for CaTiO₃

Catalyst	Probable species	Intensity (%)
Au-CaTiO ₃ (no heating)	CaAuO ₂	4.21
	TiAuO ₂	1.24
Au-CaTiO ₃ (400 °C)	CaAuO ₂	20.6
	TiAuO ₂	21.3
Au-CaTiO ₃ (600 °C)	CaAuO ₂	45.2
	TiAuO ₂	23.6
Au-CaTiO ₃ (800 °C)	CaAuO ₂	104
	TiAuO ₂	8.11

The supports were analyzed by TEM but difficulties with contrast made identification and size determination of gold particles impossible. The average particle size for the unsubstituted LaFeO₃ was found to be 43 nm and when calcium was added the average size was 107 nm. These figures are consistent with the specific surface areas measured for these samples, given the density of the perovskite material.

For CaTiO₃, The intensity of the Au(4f) peaks decreases after calcination as shown in Figs. 14 and 15 and by the calculated Au loadings in Table 2. There is no significant effect on the Ca(2p) binding energies but the O(1s) peaks had high binding energies. Often two binding energy states have been recorded for perovskites, a low BE state corresponding to lattice O²⁻ and a slightly higher BE state due to surface hydroxyl groups [33]. For LaFeO₃, the Au(4f) region is

Table 4 Data from SIMS analysis for LaFeO₃ and LaCa_xFeO₃

Catalyst	Probable species	Intensity (%)
Au-LaFeO ₃	FeAu	0.18
	FeAuO	15.5
	LaFeO ₂	2.76
	Fe ₃ AuO ₂	0.05
Au-LaCaFeO ₃ (Ca = 4 %)	CaAu	0.46
	FeAuO	10.1
	LaFeO ₂	1.58
	Ca ₂ FeAuO ₃	0.22
Au-LaCaFeO ₃ (Ca = 10 %)	CaAu	0.27
	FeAuO	7.58
	LaFeO ₂	1.68
	Ca ₂ FeAuO ₃	0.15
Au-LaCaFeO ₃ (Ca = 16 %)	CaAu	0.13
	FeAuO	2.31
	LaFeO ₂	0.93
	Ca ₂ FeAuO ₃	0.13
Au-LaCaFeO ₃ (Ca = 20 %)	CaAu	0.09
	FeAuO	2.35
	LaFeO ₂	1.07
	Ca ₂ FeAuO ₃	0.66

complicated with 2 doublets corresponding to Au⁰ and Auⁿ⁺ species. Increase in calcination led to an increase in the abundance of the cationic species, increasing from about 50 to about 70 %. We are reluctant to state definitively whether Au⁺ or Au³⁺ are present because there is an overlap in the binding energies that have been reported for these two entities. Furthermore, a degree of photoreduction of higher oxidation state gold to the zero-valent state induced by the beam in XPS work has been noted by some workers. For LaCa_xFeO₃ (Fig. 16), with 4 % Ca loading, the gold is present as Au³⁺ which transforms to metallic gold in the 10 % catalyst, with the intensity being unchanged. For the 16 and 20 % samples, the gold signal is much reduced in intensity, but with Au(4f_{7/2}) binding energies characteristic of metallic gold. There is clear evidence of calcium speciation at high calcium contents though it is difficult to draw firmer conclusions about the surface structures responsible. The speciation may be connected to the blocking behavior of calcium noted at high calcium loadings as revealed by the catalytic results and the SIMS studies (vide infra). Quantification of surface compositions for La-containing samples were made difficult by large uncertainties in the La(3d) sensitivity factor.

SIMS results

Tables 3 and 4 show SIMS data for the gold catalysts.

On increasing the calcination temperature, the gold becomes more associated with calcium than with titanium.

The SIMS results show all the probable species for CaTiO₃ and LaFeO₃. There is direct interaction between Ca and Ti for CaTiO₃. The interaction with Ca increases as the calcination temperature increases, while the interaction with Ti decreases. For LaFeO₃, there is direct interaction between Au centers and the active Fe ions but this lessens as Ca is loaded (certain Fe species present in the samples without Ca are not present in the samples with Ca, i.e., FeAu and Fe₃AuO), and, instead, there is evidence of direct interaction between Au and Ca. The intensity of signals from FeAuO and LaFeO₂ species decreases as the Ca loading is increased. Fe ions have been reported to be the active sites in Fe based perovskites and therefore Ca appears to block the active sites (with the observed decrease in activity as Ca loading increased).

Conclusions

Gold-perovskites have been prepared using a complexation method for the support. These solids are active in the low temperature oxidation of CO and some of the materials have good durability. This is particularly true of the more active AuFeTiO₃ catalysts which exhibit hardly any deactivation over a 24-h period. The activities measured are very close to those reported for the well-studied gold-titania system. Gold-

perovskites containing ionic gold combined with metallic gold seem to be more active catalysts within the range of solids we have examined. Much of the gold appears to enter the perovskite lattice in much the same way as has been seen with palladium-perovskites in the CO oxidation reaction.

Acknowledgments We thank Dr. Albert Carley from Cardiff University for the XPS analysis, Werner Jordaan from NMISA for the TOF-SIMS analysis, Rudolph Erasmus from the University of the Witwatersrand for assistance with the Raman spectroscopy and Performance Laboratories for the gold assays. We also thank MINTEK, for direct support (to LM) through Project AuTEK and the National Research Foundation, South Africa, for additional funding.

References

- Meadcroft DB (1970) Low-cost oxygen electrode material. *Nature* 226:847
- Yamazoe N, Teraoka Y (1990) Oxidation catalysis of perovskites – relationship to bulk structure and composition (valency, defects, etc.). *Catal Today* 8:175
- Kim CH, Qi G, Dahlberg K, Li W (2010) Strontium-doped perovskites rival platinum catalysts for treating NO_x in simulated diesel exhaust. *Science* 327:1624
- Royer S, Duprez D, Can F, Courtois X, Batiot-Dupeyrat C, Laassiri S, Alamdari H (2014) Perovskites as substitutes of noble metals for heterogeneous catalysis: Dream or reality. *Chem Rev* 114:10292
- Taketoshi A, Haruta M (2014) Size and structure-specificity in catalysis by gold clusters. *Chem Lett* 43:380
- Takei T, Akita T, Nakamura I, Ishida T, Haruta M (2012) Heterogeneous catalysis by gold. *Adv Catal* 55:1
- Kuwauchi Y, Yoshida H, Akita T, Haruta M, Takeda S (2012) Intrinsic catalytic structure of gold nanoparticles supported on titania. *Angew Chem Int Ed* 51:7729
- Mallick K, Scurrell MS (2003) CO oxidation over gold nanoparticles supported on titania and titania-zinc oxide: Catalytic activity due to surface modification of titania with zinc oxide. *Appl Catal A Gen* 253:527
- Boyd D, Golunski S, Heame GR, Magadzu T, Mallick K, Raphulu MC, Venugopal A, Scurrell MS (2005) Reductive routes to stabilized nanogold and relation to catalysis by supported gold. *Appl Catal A Gen* 292:76
- Yang JH, Henao JD, Raphulu MC, Wang Y, Caputo T, Grosnek AJ, Kung MC, Scurrell MS, Miller JT, Kung HH (2005) Activation of Au/TiO₂ catalyst for CO oxidation. *J Phys Chem B* 109:10319
- Mohapatra P, Moma J, Parida KM, Scurrell MS (2007) Dramatic enhancement of CO oxidation rate on Au/titania by sulphate ions. *Chem Commun* 1044
- Haruta M (2011) Role of perimeter interfaces in catalysis by gold nanoparticles. *Faraday Discuss* 152:11
- Steyn J, Patrick G, Scurrell MS, Hildebrandt D, Raphulu MC, van der Lingen E (2008) Online deactivation of gold/titania for CO oxidation in hydrogen-rich gas streams. *Gold Bull* 40:318–325
- Meilin J, Menggentuya Z, Zhaorigetu B, Yuenian S (2010) The stability study of Au/La-Co-O catalysts for CO oxidation. *Catal Lett* 134:87.164
- Liu Y, Dai H, Deng J, Li X, Wang Y, Arandiyani H, Xie S, Yang H, Guo G (2013) Au/3DOM La_{0.6}Sr_{0.4}MnO₃: Highly active nanocatalysts for the oxidation of carbon monoxide and toluene. *J Catal* 305:146
- Wei Y, Liu J, Zhao Z, Chen Y, Xu C, Duan A, Jiang G, He H (2011) Highly active catalysts of gold nanoparticles supported on three-dimensionally ordered macroporous LaFeO₃ for soot oxidation. *Angew Chemie Int Ed* 50:2326
- Uenishi M, Tanigushi M, Tanaka H, Kimura M, Nishihata Y, Mizuki J, Kobayashi T (2005) Redox behaviour of palladium at start-up in the perovskite-type LaFePdO_x catalysts showing a self-regenerative function. *Appl Catal B Environ* 57:267
- Lu H, Huang H, Liu H, Chen Y, Liu H (2008) Combustion performance of gold doping La_{0.8}Sr_{0.2}MnO₃ perovskites. *J Chem Ind Eng (China)* 59:892
- Cypes S, Hagemeyer A, Hogan Z, Weinberg WH, Yaccato K (2007) High through-put screening of low temperature CO oxidation catalysts using IR thermography. *Combin Chem High Throughput Screening* 10:25
- Galceran M, Pujol MC, Aguilo M, Diaz F (2007) Sol-gel modified Pechini method for obtaining nanocrystalline KRE(WO₄)₂ (RE = Gd and Yb). *J Sol-Gel Sci Techn* 42:79
- Huizar-Felix AM, Hernandez T, de la Parra S, Ibarra J, Kharisov B (2012) Sol-gel based Pechini method synthesis and characterization of Sm_{1-x}Ca_xFeO₃ perovskite (0.1 ≤ x ≤ 0.5). *Powder Technol* 229:290
- Shao ZP, Haile SM (2004) A high performance cathode for the next generation of solid-oxide fuel cells. *Nature* 431:170
- Shao ZP, Wang WS, Cong Y, Dong H, Tong JH, Xiong GX (2000) Investigation of the permeation behavior and stability of a Ba_{0.5}Sr_{0.5}Ca_{0.8}Fe_{0.2}O_{3-δ}. *J Membr Sci* 172:177
- Megha U, Shijina K, Varghese G (2014) Nanosized LaCo_{0.6}Fe_{0.4}O₃ perovskites synthesized by citrate sol-gel autocombination method. *Process Appl Ceram* 8:87
- Banerjee S, Choudhary VR (2000) A method for increasing the surface area of perovskite-type oxides. *Proc Indian Acad Sci (Chem Sci)* 112:535
- Silva PRN, Soares AB (2009) Lanthanum-based high surface area perovskite-type oxides and application in CO and propane combustion. *Eclat Quim* 34:31–38
- Redfern SAT (1996) High temperature structural phase transitions in perovskite (CaTiO₃). *J Phys Condens Matter* 8:8267
- Nonporous Inorganic Membranes: For Chemical Processing, eds. A. F. Sammells and M. V. Mundschaue, Wiley VCH, 2006
- Zhou K, Chen H, Tian Q, Zhu B, Shen D, Xu X (2005) Synergistic effects of palladium and oxygen vacancies in the Pd/perovskite catalysts synthesized by the spc method. *J Environ Sci (IOS Press)* 17:19
- Yakovleva IS, Isupova LA, Rogov VA, Sadykov VA (2009) Forms of oxygen in La_{1-x}Ca_xMnO_{3+δ} (x = 0–1) perovskites and their reactivity in oxidation reactions. *Kinet Catal* 49:261
- Costello CK, Kung MC, Oh HS, Wang Y, Kung HH (2004) Corrigendum to “Nature of the active site for CO oxidation on highly active Au/γ-Al₂O₃” [Appl. Catal. A Gen., 232 (2002) 159–168]. *Appl Catal A Gen* 259:131
- Costello CK, Kung MC, Oh HS, Wang Y, Kung HH (2002) Nature of the active site for CO oxidation on highly active Au/γ-Al₂O₃. *Appl Catal A Gen* 232:159
- Gonzalez A, Martinez Tamayo E, Beltran Porter A, Cortes Corberan V (1997) Synthesis of high surface area perovskite catalysts by non-conventional routes. *Catal Today* 33:361